PAPER

Check for updates

Molecular engineering of a theranostic molecule that detects Aβ plaques, inhibits Iowa and Dutch mutation Aβ self-aggregation and promotes lysosomal biogenesis for Alzheimer's disease†

Ashok Iyaswamy, [iD] ‡*[ab] Xueli Wang,‡§[c] Hailong Zhang,[c] Karthick Vasudevan,[d] Dapkupar Wankhar,[e] Kejia Lu,[a] Senthilkumar Krishnamoorthi,[a] Xin-Jie Guan,[a] Cheng-Fu Su,[a] Jia Liu,[a] Yuxuan Kan,[a] Ravindran Jaganathan,[f] Zhiqiang Deng,[a] Hung-Wing Li, [iD] *[g] Man Shing Wong [iD] *[c] and Min Li*[a]

Extracellular clustering of amyloid-β (Aβ) and an impaired autophagy lysosomal pathway (ALP) are the hallmark features in the early stages of incurable Alzheimer's disease (AD). There is a pressing need to find or develop new small molecules for diagnostics and therapeutics for the early stages of AD. Herein, we report a small molecule, namely F-SLCOOH, which can bind and detect $Aβ_{1-42}$, Iowa mutation Aβ, Dutch mutation Aβ fibrils and oligomers exhibiting enhanced emission with high affinity. Importantly, F-SLCOOH can readily pass through the blood−brain barrier and shows highly selective binding toward the extracellular Aβ aggregates in real-time in live animal imaging of a 5XFAD mice model. In addition, a high concentration of F-SLCOOH in both brain and plasma of wildtype mice after intraperitoneal administration was found. The *ex vivo* confocal imaging of hippocampal brain slices indicated excellent colocalization of F-SLCOOH with Aβ positive NU1, 4G8, 6E10 A11 antibodies and THS staining dye, affirming its excellent Aβ specificity and targetability. The molecular docking studies have provided insight into the unique and specific binding of F-SLCOOH with various Aβ species. Importantly, F-SLCOOH exhibits remarkable anti-fibrillation properties against toxic Aβ aggregate formation of $Aβ_{1-42}$, Iowa mutation Aβ, and Dutch mutation Aβ. F-SLCOOH treatment also exerts high neuroprotective functions and promotes autophagy lysosomal biogenesis in neuronal AD cell models. In summary, the present results suggest that F-SLCOOH is a highly promising theranostic agent for diagnosis and therapeutics of AD.

[a] Mr. & Mrs Ko Chi-Ming Centre for Parkinson's Disease Research, School of Chinese Medicine, Hong Kong Baptist University, Kowloon Tong, Hong Kong SAR, China. E-mail: limin@hkbu.edu.hk, ashokenviro@gmail.com, iashok@hkbu.edu.hk; Fax: +852-3411 2461; Tel: +852-3411 2919

[b] Department of Biochemistry, Karpagam Academy of Higher Education, Coimbatore, India

[c] Department of Chemistry, Hong Kong Baptist University, Kowloon Tong, Hong Kong SAR, China. E-mail: mswong@hkbu.edu.hk

[d] Manipal Academy of Higher Education (MAHE), Manipal, 576104, India

[e] Faculty of Paramedical Sciences, Assam down town University, Guwahati, Assam 781026, India

[f] Preclinical Department, Faculty of Medicine, Royal College of Medicine Perak, Universiti Kuala Lumpur, Perak, Malaysia

[g] Department of Chemistry, Chinese University of Hong Kong, Shatin, Hong Kong SAR, China. E-mail: hungwingli@cuhk.edu.hk

† Electronic supplementary information (ESI) available. See DOI: https://doi.org/10.1039/d4tb00479e

‡ Equally contributed to this work.

§ Present address: College of Pharmaceutical Sciences, Hebei University, Baoding 071002, China.

1. Introduction

Among the neurodegenerative diseases, Alzheimer's disease (AD) affects a large number of elderly people with elevated symptoms of memory loss and severely disrupts their social life.[1] AD is a progressive, complex, and multifactorial form of dementia characterized by extracellular accumulation of amyloid-β (Aβ) and intracellular accumulation of phospho-tau (p-tau) resulting in impaired cognitive symptoms.[2,3] Currently, available therapeutic agents afford only temporary relief and most of the treatment drugs being developed are highly unsuccessful in clinical trials for AD.[4,5] To date, there are no treatment strategies which can completely cure AD, detect early-stage AD symptoms or delay the AD progression.[6,7] Therefore, there is a urgent need to find new novel diagnostic agents with therapeutic properties that can be used for the detection of early stages of AD progression and can render therapeutic functions at the same time with Aβ and p-tau targeting ability.[8–10]

This journal is © The Royal Society of Chemistry 2024

J. Mater. Chem. B, 2024, **12**, 7543–7556 | 7543

Aβ is one of the hallmarks of AD progression, which self-aggregates to form oligomers and fibrils that are highly toxic to neuronal connections and synapses leading to memory loss and extracellular accumulation of Aβ plaques.[11,12] Dutch (E22Q) mutation and Iowa (D23N) mutation familial forms in AD affect the monomer Aβ folding and induce highly toxic aggregation of Aβ.[13] The accumulated insoluble Aβ oligomers or fibrils tend to form Aβ plaques causing disruption of neuronal connections in the hippocampus and activation of astrocytes and microglial cells leading to neuroinflammation.[14] During early stages of AD, soluble and insoluble Aβ accumulate in the extra neuronal spaces of the brain causing neurotoxicity and impaired autophagy.[15] Autophagy is one of the highly conserved degradative pathways for the clearance of toxic proteins like soluble and insoluble Aβ in extracellular and intracellular neuronal spaces.[16] Lysosomes also play a major role in the degradation of these toxic proteins in the formation of endolysosomes and autolysosomes in the clearance mechanism.[17] The fusion of autophagosomes and lysosomes is a major event in autophagy flux when lysosomal biogenesis is induced in the neurons and microglia during the degradative pathways.[18] During early stages of AD progression, the autophagy and lysosomal biogenesis are highly impaired and dysregulated in the neurons.[7] Therefore, early diagnosis and therapeutics are essential to slow down the progression of AD and there is a great demand for the development of theranostic small molecules/agents, which possess dual functional properties in detecting and curing or slowing down the AD progression.[10,19]

Small molecular probes such as commercially available thioflavin T (ThT) have been used for Aβ self-aggregate detection but are not highly precise in detecting Aβ oligomers or fibrils and are not blood–brain barrier permeable and highly toxic.[20] Among the existing methods of using fluorescent probes for the detection of Aβ self-aggregates, soluble and insoluble Aβ both *in vitro* and *in vivo*, certain analytical methods or fluorimetry can be used for quantitative Aβ detection and imaging.[21–26] Therefore, developing theranostic fluorescent probes with efficient blood brain barrier permeability, Aβ selectivity, accurate quantitative detection, low toxicity, therapeutic efficacy and high affinity towards both soluble and insoluble Aβ species would be a promising strategy and valuable approach for both diagnosis and drug development of AD.[27–30] Previously, we have developed NIR fluorescent probes for both soluble and insoluble Aβ species detection and *in vivo* imaging in AD models.[9,10,31,32] We have also developed a gadolinium(III) complex-cyanine molecular probe for magnetic resonance imaging (MRI) with a promising theranostic capability of diagnosis and therapy for AD.[33] In the meantime, we have recently demonstrated *in vivo* multiple therapeutic properties of the cyanine-derived theranostic agent which is low in toxicity with good blood brain barrier permeability in AD mouse models activating TFEB translocation and reducing cerebral Aβ species in a 5XFAD mouse model.[11] Therefore, cyanine dye being a versatile class of real-time turn-on fluorescent probes for Aβ imaging *in vivo*[34] has led us to further explore and investigate its novel derivatives with potentially effective diagnostic and theranostic properties.

We report herein our new development and findings of the fluoro-substituted cyanine dye, namely F-SLCOOH, which can detect Aβ fibrils and oligomers with a high binding affinity and a strong turn-on fluorescence upon binding with various Aβ species including Aβ E22Q Dutch mutation and Aβ D23N Iowa mutation. This led us to further investigate the multifunctional properties of F-SLCOOH on blood–brain barrier (BBB) permeability, Aβ selectivity, quantitative detection, toxicity, and therapeutic potential. Furthermore, we evaluated selective binding of F-SLCOOH with accumulated extracellular Aβ in real-time in live animal imaging of a 5XFAD mice model and its wild-type littermates. We also investigated whether F-SLCOOH can exhibit anti-fibrillation properties of Aβ and F-SLCOOH treatment can give neuroprotective effects and promote autophagy lysosomal biogenesis in neuronal AD cell models. Our present study has demonstrated that F-SLCOOH shows promising potential as an effective theranostic small molecule for diagnosis and treatment of AD symptoms.

2. Materials and methods

2.1. Reagents and antibodies

Dulbecco's modified Eagle's medium (DMEM) (Cat# 11965084, Gibco), Opti-MEM medium (Cat# 31985070, Gibco), fetal bovine serum (FBS) (Cat# 10500064, Gibco), protease inhibitors (Cat# HY-K0011, MedChemExpress), phosphatase inhibitors (Cat# A32957, Pierce), BCA assay reagent (Cat# 23225, Pierce), and Torin1 (Cat# 2273) were purchased from BioVision. Chloroquine (CQ) (Cat# C6628) was purchased from Sigma-Aldrich. Alexa Fluor 488 Goat Anti-Mouse IgG (Cat# A11001) was purchased from Life Technologies. Cryomatrix (Cat# 6769006, Thermo Scientific), medical X-ray film (Cat# CK04, FUMING-WEI), paraformaldehyde (PFA) (Cat# P6148), PVDF membrane (Cat# 10600023), fluorescence mounting media (Cat# S3023), thioflavine S (Cat# T1892, Sigma), and LysoTracker® Green DND-99 (Cat# L-7528), and details of the primary antibodies used in this study including 4G8 antibody (Cat# 800705, Biolegend, United Kingdom), 6E10 antibody (Cat# 803003, Biolegend, United Kingdom), anti-amyloid beta oligomer (NU1), and anti-oligomer-A11 (AHB0052) were purchased from Abcam and Cell Signalling Technologies.

2.2. Aβ$_{1-42}$ stock solution preparation

1 mg Aβ powder was dissolved in the mixed solution of 500 μL hexafluoroisopropanol and 500 μL trifluoroacetic acid. Then it was ultrasonicated for 4 hours and vortexed for 4 hours in turn and left overnight at room temperature. The stock solution should be stored at −20 or −80 °C in a deep freezer.[33]

2.3. The Aβ fibril, oligomer and monomer

Around 135.45 μL of storage solution was vacuum dried and added to 20 μL 0.02% NH$_3$–H$_2$O and 80 μL 10 mM HCl. The 300 μM Aβ fibril was prepared by incubating the Aβ$_{1-42}$ monomer at 37 °C for 72 h; while the 300 μM Aβ oligomer was prepared by incubating the Aβ$_{1-42}$ monomer at 4 °C for 72 h.

7544 | *J. Mater. Chem. B*, 2024, **12**, 7543–7556

This journal is © The Royal Society of Chemistry 2024

Aβ monomers were prepared by dissolving the powder directly to the experimental concentration using phosphate buffer. All three peptides of Aβ$_{1-42}$, Iowa mutation Aβ and Dutch mutation Aβ used the same method to prepare the fibrils, oligomers and monomers.[33]

2.4. Fluorescence spectra measurement

Fluorescence spectra were measured using a FM-4 fluorescence spectrometer (Horiba FluoroMax-4 photoluminescence spectrometer) after the same concentration of dye was mixed with different concentrations of protein for 10 minutes. The saturation binding curves were fitted with Origin software.[33]

2.5. Cell culture

Neuroblastoma cells (N2a), hippocampal neuronal cells (HT-22), and HeLa-tf-LC3 (mRFP-EGFP-LC3) stable cells were used in our research studies. The cells were cultured in standard medium DMEM, supplemented with 5–10% fetal bovine serum (FBS), and 1% penicillin–streptomycin (PSN) solution.[35]

2.6. Cell viability assay (MTT test)

N2a cells was cultured in the 48-well plate and after 24 hours, the cells were treated with F-SLCOOH at different concentrations for 24 to 48 hours incubation, MTT (5 mg mL^{-1} in DMSO) solution was mixed in each well with cells at 37 °C for 4 hours and the reaction was stopped by adding DMSO. Then the plate was mildly vortexed for a few seconds to mix the reaction mixture thoroughly and then incubated at 37 °C overnight and finally read in a microtiter plate reader at an absorbance of 570 nm.[16]

2.7. Anti-fibrillation thioflavin T assay

We prepared a stock solution of Aβ$_{1-42}$, Iowa mutation Aβ and Dutch mutation Aβ for the anti-fibrillation assay. All these Aβ peptides were aliquoted in different tubes at various concentrations with or without F-SLCOOH in the phosphate buffer and Aβ peptides of Aβ$_{1-42}$, Iowa mutation Aβ and Dutch mutation Aβ. The tubes with the peptides and F-SLCOOH at 37 °C for 48 to 72 hours with mild shaking. After the incubation period, the Aβ peptides with or without F-SLCOOH tubes were mixed with thioflavin T for 10 minutes in the dark. Iowa mutation Aβ, Dutch mutation Aβ and Aβ$_{1-42}$ fibril aggregation was measured with an excitation at 440 nm and emission at 480 nm using a fluorescence microplate reader (Pekin Elmer, U.S).[11]

2.8. Confocal imaging of Aβ fibrils

Iowa mutation Aβ, Dutch mutation Aβ and Aβ$_{1-42}$ prepared fibrils with or without F-SLCOOH were mixed with thioflavin T for 10 minutes in the dark. The complete fibril solution with or without F-SLCOOH was examined using a confocal laser scanning microscope (Leica TCS SP8). The images of the green fluorescence of the fibrils were compared between control Aβ with or without F-SLCOOH for its anti-fibrillation effect.[33]

2.9. Autophagy flux experiment

The HeLa-tf-LC3 (mRFP-EGFP-LC3) stable cells in the coverslip were cultured in a 24-well plate with standard medium DMEM supplemented with 5–10% fetal bovine serum (FBS) and 1% penicillin–streptomycin (PSN) solution. After 24 hours of cell incubation, the cells were treated with F-SLCOOH, Torin1 and CQ for 24 hours. After 24 hours of treatment, the cells were fixed with 4% PFA and the cells were embedded into the slides using mounting medium. mRFP-EGFP-LC3 was examined using a confocal laser scanning microscope (Leica TCS SP8) and evaluated for autophagy flux.[11]

2.10. TEM imaging

N2a and HT-22 were cultured in a 12-well plate with standard medium DMEM supplemented with 5–10% fetal bovine serum (FBS) and 1% penicillin–streptomycin (PSN) solution. The cells were treated with F-SLCOOH and Torin1. After 24 hours, the cells were fixed with 2.5% glutaraldehyde in 0.1 M sodium cacodylate buffer for 1 hour at room temperature. The dehydrated cells were embedded in Poly/Bed® 812 for ultra-thin slicing to examine the autolysosomes in treated cells and viewed under a Philips CM100 transmission electron microscope at the QMH Electron Microscope Unit, Queen Mary Hospital, University of Hong Kong, Hong Kong.[11]

2.11. Lysotracker imaging and flow cytometry

N2a and HT-22 in the coverslip were cultured in 12- or 24-well plates with standard medium DMEM supplemented with 5–10% fetal bovine serum (FBS) and 1% penicillin–streptomycin (PSN) solution. After 24 hours of cell incubation, the cells were treated with F-SLCOOH and Torin1. After 24 hours treatment, the cells were incubated with LysoTracker® Green DND-99 for 1 to 2 hours. The cells were then fixed with 4% PFA and embedded in the slides using mounting medium. The lysotracker was examined using a confocal laser scanning microscope (Leica TCS SP8) and the lysotracker positive cells were evaluated using flow cytometry (BD Accuri C6 Plus Flow Cytometer).[11]

2.12. Immunohistochemistry

After the specific time point, the animals were trans-cardiac perfused with 1XPBS and 4% paraformaldehyde (PFA) to remove the blood content in the organs and brain. The brain was extracted from the skull of the head and incubated in 4% PFA at 4 °C for 24–48 hours. Then the brains were washed in 1XPBS and incubated in 30% sucrose until sinking into the solution at 4 °C for the cryo-sectioning. The hippocampal brain slices were sectioned in the cryotome and subjected to floating immunohistochemistry staining. The brain slices were incubated with the Aβ fibrils and oligomer positive primary antibodies such as 6E10, NU1, 4G8, A11 and thioflavin-S (Thio-S) for staining.[17] The fluorescence images were examined using a confocal laser scanning microscope (Leica TCS SP8).

This journal is © The Royal Society of Chemistry 2024

J. Mater. Chem. B, 2024, **12**, 7543–7556 | 7545

2.13. Molecular docking and binding pattern of F-SLCOOH

The PDB structure of monomer Aβ (1IYT), fibril Aβ (5OQV), and oligomer Aβ (6RHY) was retrieved from the protein data bank. The Dutch and Iowa mutation were induced using Swiss PDB Viewer. We employed a molecular docking approach to investigate the interaction between target proteins Iowa mutation Aβ, Dutch mutation Aβ and $A\beta_{1-42}$ with F-SLCOOH. The 3D structure of all the proteins was retrieved from PDB (PDB ID: 5OQV). We used AutoDockTools (version 1.5.6) to add hydrogen atoms and compute Kollman charges. We reviewed the literature evidence and the Metapocket server (https://metapocket. eml.org/) to locate the binding. Additionally, we converted target protein and compound pdb files to pdbqt files. We then performed further molecular docking analysis using AutoDock Vina. To ensure the consistency of the docking results, we repeated the docking process to determine the optimal binding pose. Finally, we created a schematic representation of the intermolecular interactions and binding mode using BIOVIA Discovery Studio v.2021 and Chimera v.1.16.

2.14. Animal experiments

Wild type C57BL/6 and 5XFAD mice were used in the research experiments of this study. All animal experiments were performed in accordance with the relevant guidelines and regulations of HASC. All animal experiments were approved by the Hong Kong Baptist University Committee on the Use of Human and Animal Subjects in Teaching and Research (HASC approval #HASC/20–21). The researchers who performed all the experiments got approval from the Department of Health for performing the animal experiments in Hong Kong under the licence (20–28) in DH/HT&A/8/2/6 Pt.1.

2.15. Real time *in vivo* imaging of F-SLCOOH

Wild type C57 and 5XFAD mice were used for the real time *in vivo* imaging of F-SLCOOH in live animal brains. The 5XFAD or WT mice were injected with the F-SLCOOH (100 to 300 μl) by intravenous administration *via* the tail vein. The animal was anesthetised using chloral hydrate (5–8%) and subjected to real time live animal imaging in the brain. At different time points, the animals were pictured for the fluorescent signals in real time live animal imaging (λ_{ex} = 465 nm, λ_{em} = 575–650 nm) using a small animal imaging system (IVIS XR). The relative fluorescence signals of F-SLCOOH [F(t)/F(pre)] in the brain of 5XFAD and WT mice were recorded.[33]

2.16. F-SLCOOH concentration in brain and plasma

Wild type C57BL/6 mice were intraperitoneally injected with F-SLCOOH (10 mg kg^{-1}) for the detection of bioavailable F-SLCOOH in the brain and plasma at different timepoints (0, 30, and 60 min). The concentration of the F-SLCOOH was determined using Triple Quad LC/MS 6460 (Agilent Technologies) in the brain and plasma of C57BL/6 mice. The HPLC profiling of F-SLCOOH was detected using UHD Accurate-Mass Q-TOF LC/MS (Agilent Technologies).

2.17. Statistical analysis

All data in this study were statistically analyzed using GraphPad Prism software. The results are reported as mean ± SEM with the number of samples as mentioned in the Methods section or figure legends. The treatment groups were statistically compared using one-way analysis of variance (ANOVA) with subsequent Dunnett's or Tukey or Bonferonni multiple comparison among groups and control groups with *post hoc* analysis. Each experiment datum is represented as 3 independent replicates.

3. Results

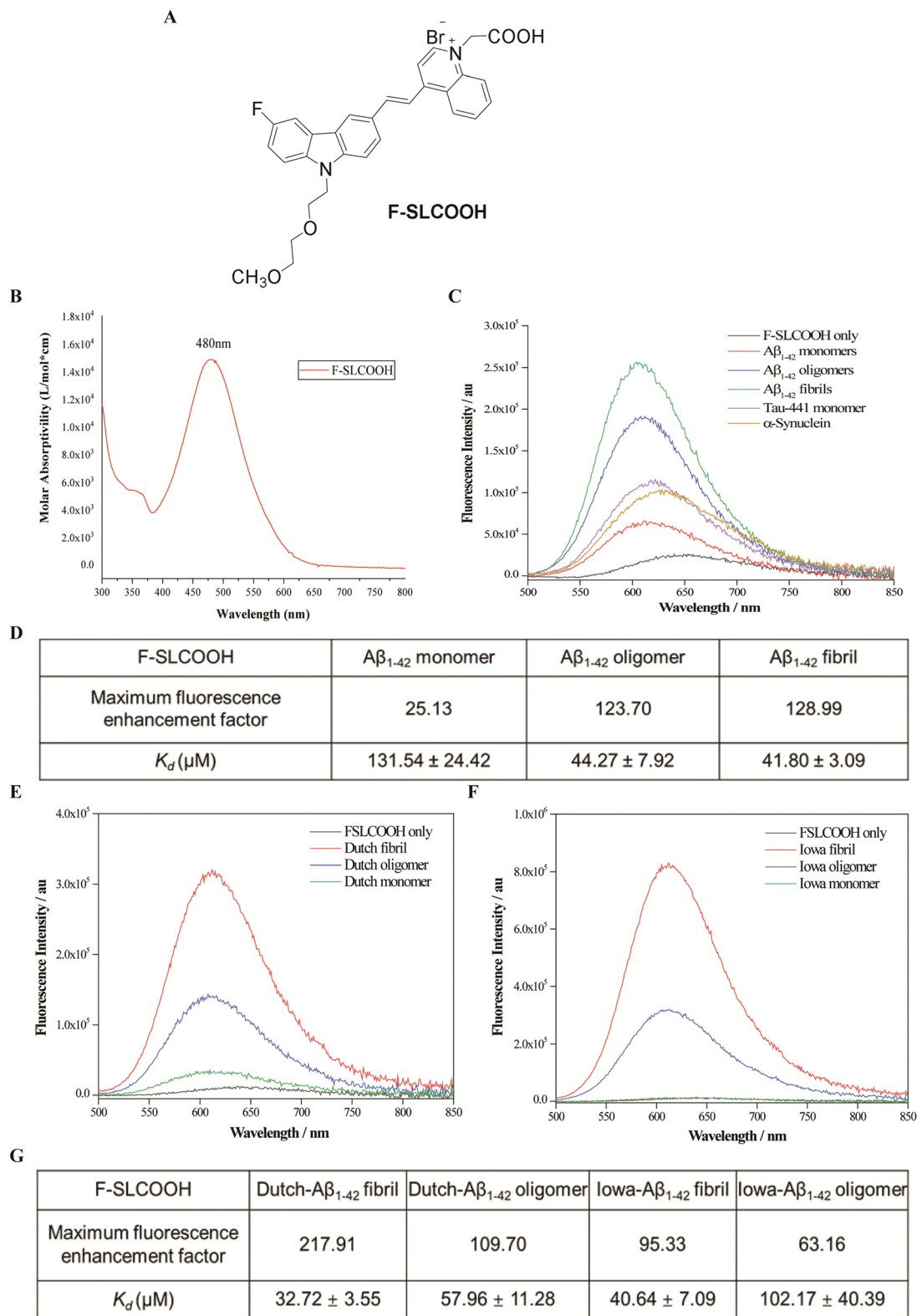### 3.1. Structure and optical properties of F-SLCOOH

To increase the lipophilicity of a cyanine dye and enhance its BBB penetrability, the strategy of fluoro-substitution was adopted to develop the theranostic molecule. The synthetic route of the theranostic molecule F-SLCOOH is outlined in Scheme S1 (ESI†). The chemical structure of F-SLCOOH (Fig. 1A) was confirmed *via* ^{1}H (Fig. S1, ESI†), ^{13}C (Fig. S2, ESI†) nuclear magnetic resonance (NMR) spectroscopy and high-resolution mass spectroscopy (HRMS) (Fig. S3, ESI†). F-SLCOOH shows a strong absorption peak at 480 nm in pH 7.4 phosphate buffer solution and a weak emission band at 645 nm upon excitation (Fig. 1B). F-SLCOOH exhibits strong fluorescence enhancement towards various $A\beta_{1-42}$ species including fibrils, oligomers and monomers with an enhancement factor over 100 times. The fluorescence enhancements are much stronger for Aβ than those of tau aggregates and α-synuclein (Fig. 1C). To investigate the binding affinity of F-SLCOOH with Aβ species, we performed the fluorescence titration of them (Fig. S4–S6, ESI†) in phosphate buffer (pH = 7.4). Based on the Scatchard plot analysis, the dissociation constants (K_d) of F-SLCOOH with $A\beta_{1-42}$ fibril, oligomers and monomer are in the range of 44–61 μM (Fig. 1D). In addition, F-SLCOOH showed much stronger binding affinity toward Iowa mutation Aβ and Dutch mutation Aβ fibrils as revealed in the fluorescence titration (Fig. 1E and F) and the respective Scatchard plot analysis (Fig. S7–S11, ESI†) with K_d of 41 and 33 μM for Iowa mutation Aβ and Dutch mutation Aβ fibrils, respectively, which are tabulated in Fig. 1G. We also investigated the fluorescence response of F-SLCOOH in the presence of various bioactive small molecules and metal ions (Fig. S13, ESI†) including valine, aspartic, arginine, phenylalanine, Mg^{2+}, Ca^{2+}, Hg^{2+}, Cu^{2+}, Ag^+, K^+, and Zn^{2+}, with which the fluorescence intensity was insignificantly affected, suggesting its good selectivity toward Aβ. Furthermore, F-SLCOOH was found to be photostable under ambient light illumination over a period of time (Fig. S14, ESI†) and its fluorescence was stable over a wide range of pH values (Fig. S15, ESI†). In short, the above results signify that F-SLCOOH is a potentially useful fluorescent probe for real-time detection and visualization of Aβ in an animal model for diagnosis of AD.

3.2. Real time detection and imaging of F-SLCOOH in a preclinical Alzheimer's disease mouse model

To be practically useful for real time detection and imaging of Aβ plaques in preclinical Alzheimer's disease mouse models,

7546 | *J. Mater. Chem. B*, 2024, **12**, 7543–7556

This journal is © The Royal Society of Chemistry 2024

Fig. 1 Structure and optical properties of F-SLCOOH. (A) Chemical structure of F-SLCOOH. (B) Absorption spectrum of F-SLCOOH (20 μM), measured in pH 7.4 phosphate buffer solution. (C) Fluorescence spectra of F-SLCOOH (10 μM) in the presence of 10 μM $A\beta_{1-42}$ species (monomers, oligomers and fibrils), Tau-441 aggregation and α-synuclein in 25 mM phosphate buffer (pH = 7.4). (D) The table summarizes the fluorescence enhancement factor and dissociation constant (K_d) of F-SLCOOH (2 μM) with $A\beta_{1-42}$ fibril, oligomers and monomer in 25 mM phosphate buffer (pH = 7.4). (E) Fluorescence spectra of F-SLCOOH (10 μM) in the presence of 10 μM E22Q DUTCH Aβ mutation (monomers, oligomers and fibrils) in 25 mM phosphate buffer (pH = 7.4). (F) Fluorescence spectra of F-SLCOOH (10 μM) in the presence of 10 μM Asn23 IOWA Aβ mutation (monomers, oligomers and fibrils) in 25 mM phosphate buffer (pH = 7.4). (G) The table summarizes the fluorescence enhancement factor and dissociation constant (K_d) of F-SLCOOH (2 μM) with E22Q DUTCH and Asn23 IOWA Aβ mutation fibril and oligomers in 25 mM phosphate buffer (pH = 7.4).

This journal is © The Royal Society of Chemistry 2024

J. Mater. Chem. B, 2024, **12**, 7543–7556 | **7547**

the Aβ-targeted fluorescent probe needs to be penetrate the BBB. To test this ability of F-SLCOOH in animal models, we assessed the real time detection and imaging of F-SLCOOH in a preclinical Alzheimer's disease mouse model (5XFAD) and compared the results with a wildtype (WT) mouse. To investigate the BBB permeability of F-SLCOOH in animal brain, 5XFAD and WT mice were injected with the F-SLCOOH (100 μL of 10 mg kg^{-1}) in PBS (0.5 M, pH = 7.4) and 10% DMSO *via* the tail-vein. The live animals were imaged in the IVIS spectrum *in vivo* imaging system, the fluorescence spectra of the F-SLCOOH were captured and their respective fluorescence signals were monitored in real time. The F-SLCOOH treated 5XFAD and WT mice showed bright fluorescence signals at all time points, clearly demonstrating that F-SLCOOH is highly BBB permeable (Fig. 2A and B) and can reach the accumulated target Aβ fibrils and oligomers of senile plaques in 5XFAD (λ_{ex} = 465 nm, λ_{em} = 575–650 nm). We also found that the fluorescence signals of F-SLCOOH was much enhanced in a 5XFAD preclinical Alzheimer's disease mouse model as compared to those of the WT mouse model at all time points. The results signify that F-SLCOOH has high affinity toward the deposition of Aβ fibrils and oligomers leading to enhanced fluorescence emission in all time points and higher retention of F-SLCOOH in the brains of the 5XFAD mouse model as compared to those of the WT mouse model. These results are given in the graphical plot of the relative fluorescence signals of F-SLCOOH [F(t)/F(pre)] in the brain of 5XFAD and WT mice over time after the injection for each time point (Fig. 2C). To confirm the BBB permeability of the cyanine dye, we investigated the level of F-SLCOOH in the brain and plasma of WT mice (C57/BL6) at different time points such as 0, 30 and 60 minutes after being intraperitoneally injected with F-SLCOOH (10 mg kg^{-1}) using the LC-MS method (Fig. S18 and S19, ESI†). As expected, a high concentration of F-SLCOOH was found in the brain and plasma at both time points and the F-SLCOOH concentration was higher at 60 rather than 30 minutes illustrating that F-SLCOOH is highly bioavailable in the brain for its theranostic function. Taken together, the above results reveal that F-SLCOOH can readily cross the BBB and has high selective binding toward Aβ fibrils and oligomers affording enhanced and bright fluorescence signals at all time points in the real time detection and diagnosis in a preclinical Alzheimer's disease mouse model.

3.3. Confocal imaging of F-SLCOOH in hippocampal brain slices of the preclinical 5XFAD mouse model

To evaluate the detection and labelling ability of F-SLCOOH toward Aβ fibrils and oligomers in the hippocampal brain slices of a preclinical 5XFAD and WT mouse model, we injected
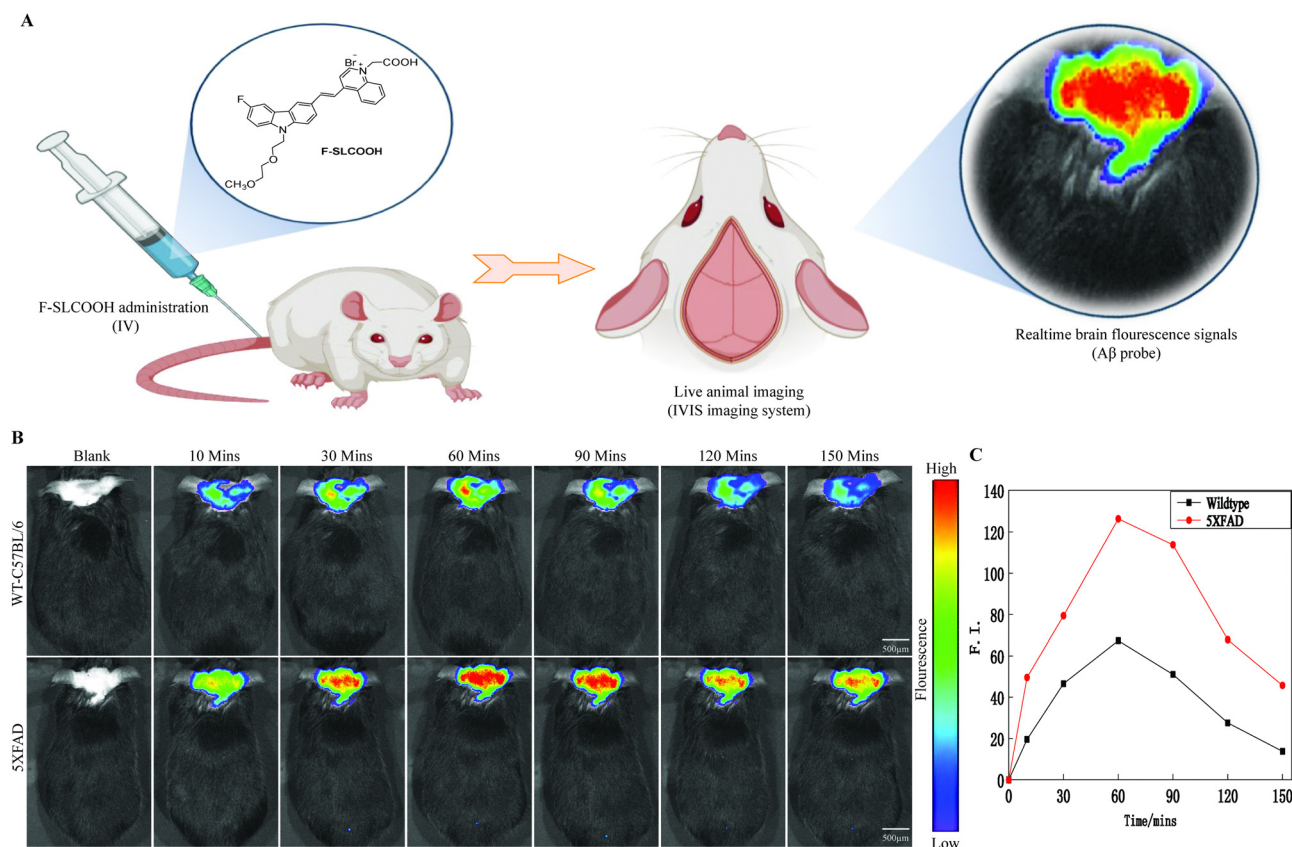
Fig. 2 Realtime imaging of F-SLCOOH in a preclinical Alzheimer's disease mouse model. (A) Schematic representation of the F-SLCOOH imaging properties in animal models. (B) *In vivo* images of 5XFAD and WT mice injected with the F-SLCOOH (100 μL of 10 mg kg^{-1}) in PBS (0.5 M, pH = 7.4) and 10% DMSO *via* the tail-vein and their respective fluorescence signals were monitored in real-time (λ_{ex} = 465 nm, λ_{em} = 575–650 nm). (C) The plots of the relative fluorescence signals of F-SLCOOH [F(t)/F(pre)] in the brain of 5XFAD and WT mice over time after the injection.

7548 | *J. Mater. Chem. B*, 2024, **12**, 7543–7556

This journal is © The Royal Society of Chemistry 2024

F-SLCOOH (100 μL of 10 mg kg^{-1}) in PBS (0.5 M, pH = 7.4) and 10% DMSO was intravenously administered in WT and 5XFAD mice *via* the tail-vein. The hippocampal brain slices were sectioned in the cryotome and subjected to floating immuno-histochemistry staining. The brain slices were incubated with the Aβ fibril- and oligomer-positive primary antibodies such as 6E10, NU1, 4G8, A11 and thioflavin-S (Thio-S) staining dye. The Aβ fibrils specific Thio-S staining was colocalised well with F-SLCOOH in the central and peripheral areas of the hippo-campus and other regions of the 5XFAD brain as compared to those of the WT mice brain (Fig. 3A and B). From the Thio-S staining colocalization experiment, it is clearly shown that F-SLCOOH exhibits high selectivity and specificity toward Aβ fibrils. Besides, Aβ oligomers specific primary antibodies NU1 and A11 showed very good colocalization with F-SLCOOH in the central and peripheral regions of the hippocampus in the 5XFAD brain as compared to those of the WT mice brain (Fig. 3A and B). These results clearly illustrate that the fluores-cence of F-SLCOOH colocalizes with Aβ oligomer specific primary antibodies in immunohistochemistry experiments. We also carried out immunohistochemistry staining with Aβ specific primary antibodies namely 6E10 and 4G8, which can detect Aβ monomers, oligomers, and fibrils. The fluorescence of F-SLCOOH showed very good colocalization with Aβ specific primary antibodies, 6E10 and 4G8 in the hippocampus of the 5XFAD brain in contrast to those of the WT mice brain

(Fig. 3A and B). The fluorescence intensity plots of F-SLCOOH colocalized with several Aβ targeting antibodies in the hippo-campus of the 5XFAD brain as compared to those of the WT mice brain are given in Fig. 3C.

Taking all these results together, they consistently demon-strate that F-SLCOOH can efficiently bind with Aβ fibrils, oligomers and monomers in the central and peripheral Aβ plaques of the hippocampus in 5XFAD brain regions.

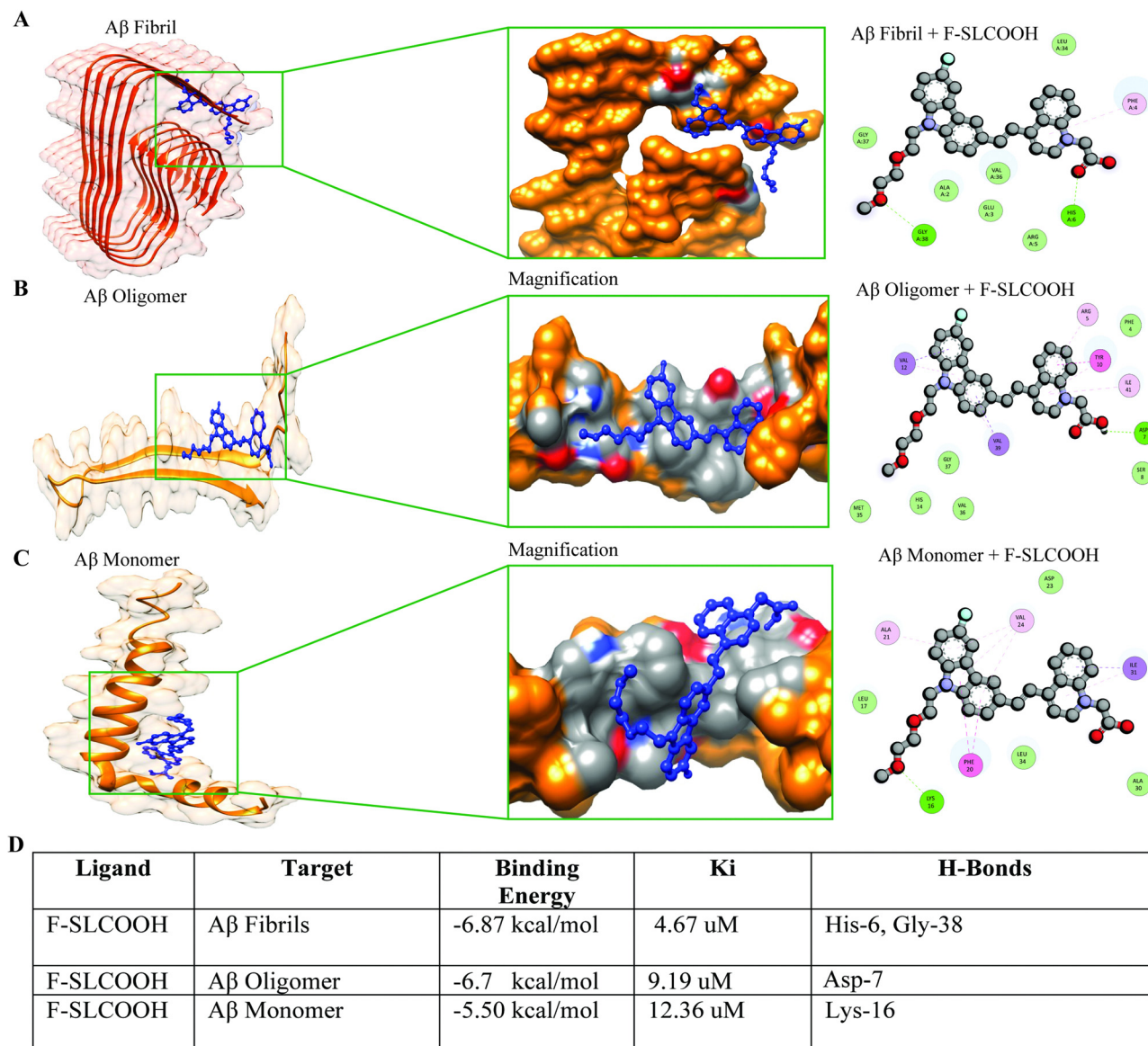### 3.4. Molecular docking and binding patterns of F-SLCOOH with Aβ ligand binding domains

To validate the efficient binding of F-SLCOOH with Aβ fibrils, oligomers and monomers protein binding domain, we carried out molecular docking to determine the binding affinity between the Aβ targets and F-SLCOOH. We performed docking analysis using the AutoDock software program. The docking analysis was repeated several times to minimize the inconsis-tency and bias in the results. F-SLCOOH was observed to have significantly higher binding affinities with fibrils and oligo-mers than with monomers, suggesting potential interactions with these targets in the docking results (Fig. 4A–C). Further-more, it is also noteworthy that fibrils and oligomers were able to establish hydrogen bond interactions with the compound as well (Fig. 4D). Specifically, F-SLCOOH experienced a strong hydrogen bonding interaction with fibril residues, demonstrat-ing efficient and reliable binding. The critical interacting
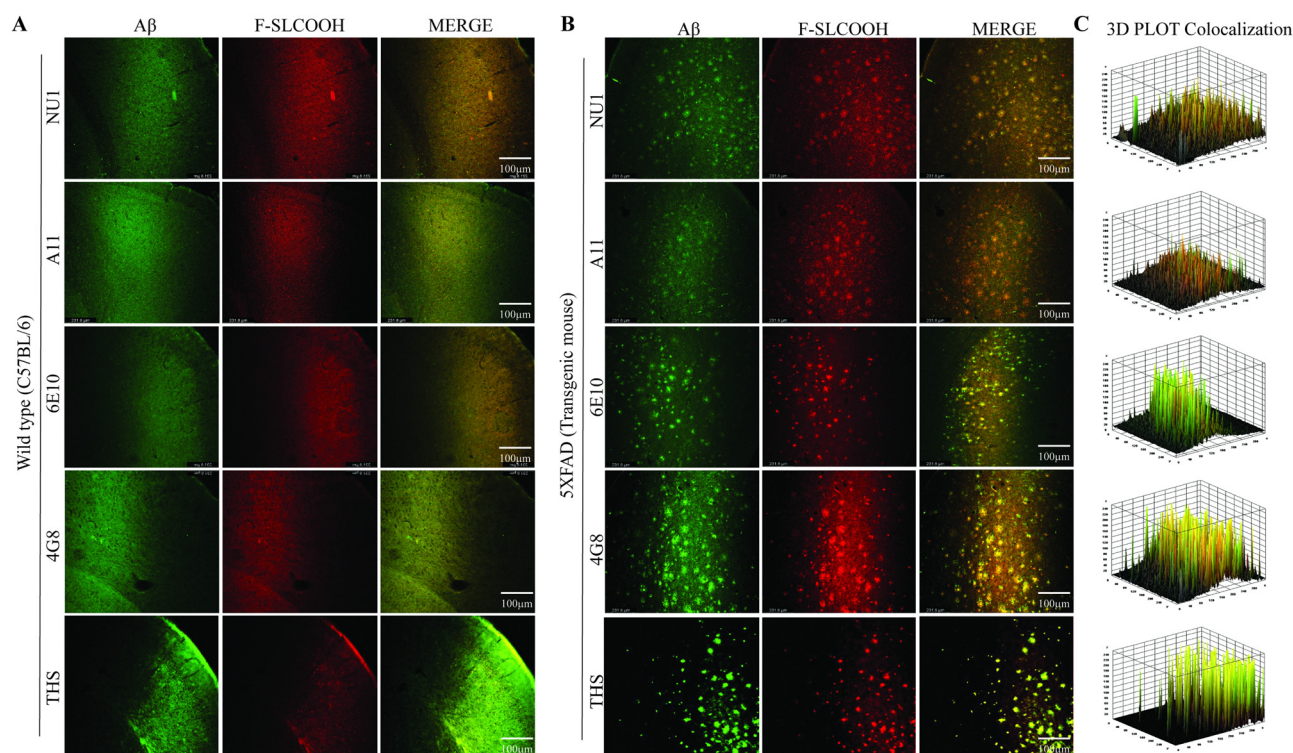
Fig. 3 Confocal microscopic images of F-SLCOOH in hippocampal brain slices of a preclinical Alzheimer's disease mouse model. F-SLCOOH was intravenously administered in (A) WT and (B) 5XFAD mice *via* the tail-vein. Hippocampal brain sections of (A) WT and (B) 5XFAD mice were labelled with F-SLCOOH *in vivo* examined *via* confocal microscopic and *ex vivo* imaging followed by incubation with a primary antibody (6E10, NU1, 4G8 and A11) with a secondary antibody conjugated with Alexa 488 and thioflavin-S (Thio-S) staining, respectively. (C) The 3D plot graphs displaying the colocalization of F-SLCOOH with the corresponding Aβ antibodies and staining agent in 5XFAD mice hippocampal brain slices.

Fig. 4 Molecular docking and binding pattern of F-SLCOOH with Aβ ligand binding domains. The comparison of docking results with $A\beta_{1-42}$ fibril, oligomer and monomer LBD and binding pattern of F-SLCOOH. Binding pattern of F-SLCOOH with the ligand binding domain of $A\beta_{1-42}$ (A) fibril, (B) oligomer and (C) monomer. Residues of $A\beta_{1-42}$ fibril, oligomer and monomer interacting with F-SLCOOH are given in the marked pictures with the ligand binding domain of Aβ. (D) The table reveals the binding energy, Ki, H-bonds of the ligand target residues of $A\beta_{1-42}$ fibril, oligomer and monomer interacting with F-SLCOOH.

residues and binding mode of F-SLCOOH to the targets are shown in the figures (Fig. 4A–C). In familial AD, E22Q Dutch and D23N Iowa mutations cause most toxic Aβ fibrils and highly pathogenic forms of AD.[13] Therefore, we confirmed whether, F-SLCOOH has significantly higher binding affinities with Iowa mutation Aβ and Dutch mutation Aβ fibrils and oligomers than with monomer, suggesting potential interactions with these targets in the docking results (Fig. S17A–F, ESI†). On the other hand, molecular docking of F-SLCOOH with p-Tau and α-Syn did not show strong ligand binding and the docking binding affinity with -6.0 kcal mol^{-1} for p-Tau + F-SLCOOH and -5.5 kcal mol^{-1} for α-Syn + F-SLCOOH (Fig. S21, ESI†) as compared to those of Aβ species with

F-SLCOOH. Taken together, these data consistently demonstrated that F-SLCOOH can efficiently bind with Aβ fibrils and oligomers more consistently than the monomers binding domain, as illustrated in molecular docking and binding patterns of F-SLCOOH.

3.5. Therapeutic potential and anti-fibrillation properties of F-SLCOOH with Aβ

To investigate the therapeutic potential of F-SLCOOH in a neuroblastoma (N2a) cell model, we first tested the cytotoxicity of F-SLCOOH in the N2a cells using MTT assay and LDH assay. We found that the lethal concentration 50 (LC_{50}) of F-SLCOOH in the N2a cells was >200 μM and the LDH assay did not show

7550 | *J. Mater. Chem. B*, 2024, **12**, 7543–7556

This journal is © The Royal Society of Chemistry 2024

much toxicity upon treatment with different concentrations of F-SLCOOH. Both the MTT assay and LDH assay (Fig. 5A and B)

revealed that even a high concentration of F-SLCOOH was highly tolerable in the cultured cells and biocompatible with
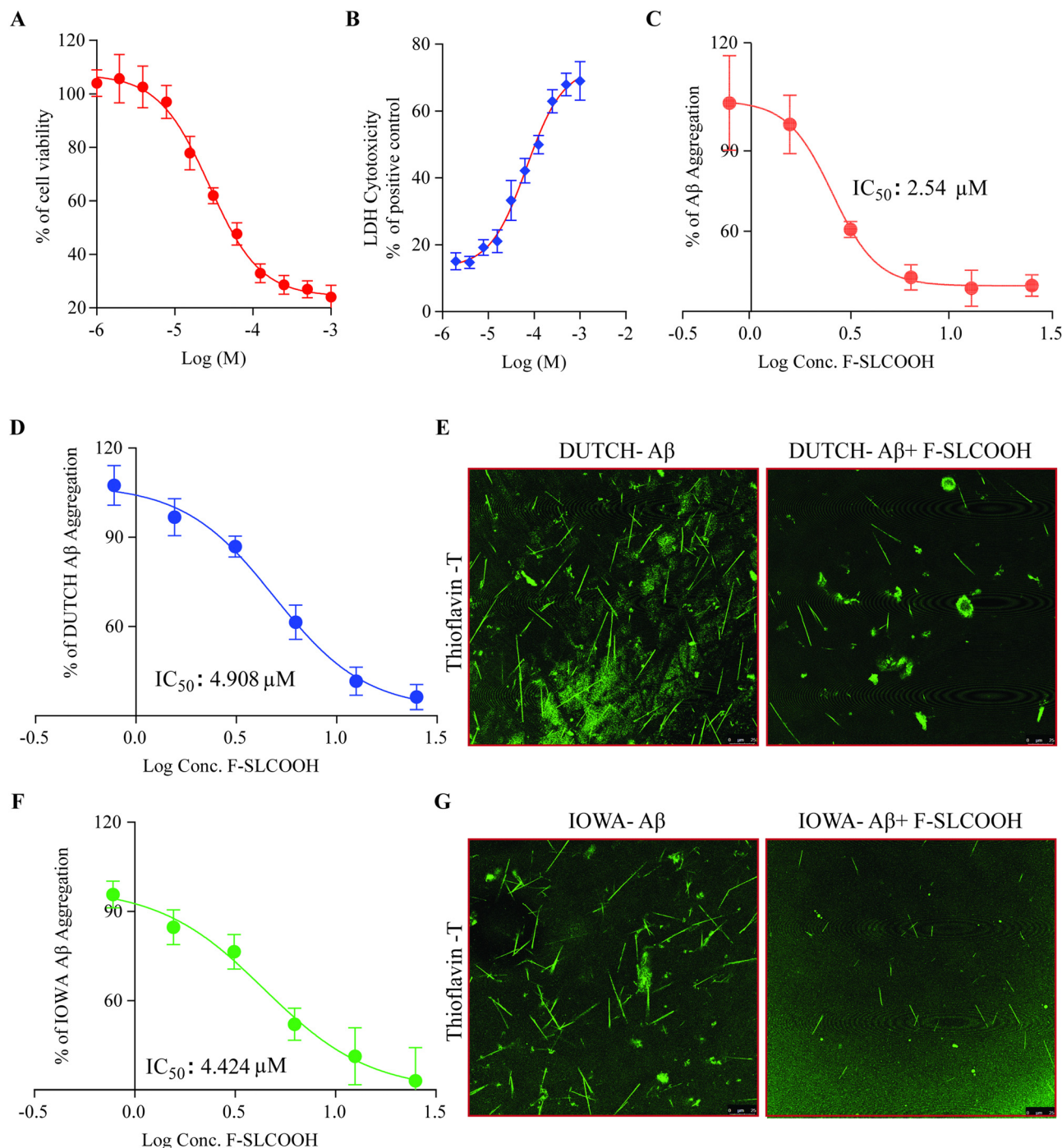
Fig. 5 Cytotoxicity and anti-fibrillation properties of F-SLCOOH with Aβ. (A) The cytotoxicity of F-SLCOOH was determined using a cellular viability MTT assay in N2A cells. (B) Cytotoxicity or cell death after the treatment of F-SLCOOH was determined using an LDH assay with N2A cells. (C) F-SLCOOH dose dependently inhibited the fibril formation of Aβ in the anti-Aβ fibrillation assay using ThT fluorescence. The IC_{50} value of the anti-fibrillation activity of F-SLCOOH is 2.54 μm. (D) F-SLCOOH dose dependently inhibited the fibril formation of E22Q DUTCH Aβ mutation in the anti-Aβ fibrillation assay using ThT fluorescence. The IC_{50} value of the anti-fibrillation activity of F-SLCOOH is 4.908 μm. (E) Confocal imaging of fibril formation of E22Q DUTCH Aβ mutation and F-SLCOOH inhibition using ThT fluorescence. (F) F-SLCOOH dose dependently inhibited the fibril formation of Asn23 IOWA Aβ mutation in the anti-Aβ fibrillation assay using ThT fluorescence. The IC_{50} value of the anti-fibrillation activity of F-SLCOOH is 4.424 μm. (G) Confocal imaging of the fibril formation of Asn23 IOWA Aβ mutation and F-SLCOOH inhibition using ThT fluorescence. Each data point represents the average of three replicates and the data are represented as the mean ± SEM.

This journal is © The Royal Society of Chemistry 2024

J. Mater. Chem. B, 2024, 12, 7543–7556 | 7551

insignificant toxicity, which would be beneficial for other biological applications. To explore further the biological benefits of F-SLCOOH, we investigated the Aβ anti-fibrillation properties of F-SLCOOH to see whether it can act as an inhibitor against the Aβ aggregates formation. Then, we performed a ThT-labelled fluorescence assay using an Aβ (Aβ$_{1-42}$) seeding method at different concentrations and studied it at different time points. F-SLCOOH treatment revealed an efficient Aβ anti-fibrillation property, effectively suppressing the Aβ aggregates and Aβ fibril formation. The IC$_{50}$ value of anti-fibrillation activity of F-SLCOOH (Fig. 5C) was found to be 2.54 μm, which clearly illustrates that even at a low concentration, F-SLCOOH can deliver promising potential for therapeutics of AD. Additionally, the anti-fibrillation activity of F-SLCOOH were further assured by the dot blot study (Fig. S23, ESI†) consistently demonstrating its therapeutic value and efficacy. As anticipated, F-SLCOOH also clearly demonstrated an efficient Aβ anti-fibrillation effect with an IC$_{50}$ value of 4.424 and 4.908 μm for Iowa mutation Aβ and Dutch mutation Aβ, respectively (Fig. 5D and F). These results were further confirmed in the confocal imaging of their fibril formation in the absence and presence of F-SLCOOH (Fig. 5E and G). Furthermore, Aβ$_{1-42}$ fibrils, Iowa mutation Aβ fibrils and Dutch mutation Aβ fibrils treatment in SH-SY5Y cells caused morphological changes and reduced cell growth; however, treatment of F-SLCOOH rescued the morphological changes and increased SH-SY5Y cell growth (Fig. S25, ESI†). Apart from the low toxicity and anti-fibrillation properties of F-SLCOOH, we investigated whether it could exhibit neuroprotection properties in N2a cells. We carried out treatment of the F-SLCOOH against Aβ$_{1-42}$ monomers, oligomers, and fibril-induced cytotoxicity in neuronal cells. After the treatment with F-SLCOOH in the presence of Aβ in neuronal cells (Fig. S10A, ESI†), F-SLCOOH demonstrated excellent neuroprotection and rescued the neuronal cells from the cytotoxicity induced by the Aβ$_{1-42}$ monomers, oligomers, and fibrils. In addition, when Aβ accumulated in the intracellular or extracellular space in the form of aggregates or fibrils, it can induce excessive formation of reactive oxygen species (ROS), which is highly toxic in inducing oxidative stress, apoptosis and neuronal death in the brain. Therefore, we evaluated whether F-SLCOOH has the ability to eradicate the Aβ-induced ROS in the neuronal cells. We found that F-SLCOOH treatment can significantly reduce the ROS levels in the neuronal cells pre-treated with the Aβ$_{1-42}$ monomer, oligomers and fibrils (Fig. S10B, ESI†) in the *in vitro* experiments. Meanwhile, F-SLCOOH can protect the neuronal cells to withstand the ROS induced toxicity and readily reduce their toxicity levels and ROS generation (Fig. S16A and B, ESI†). Moreover, in the study of *in vivo* acute toxicity of F-SLCOOH in WT (C57BL/6), the mice did not show any significant changes in animal behaviour, body weight, and organ weight and did not exhibit any histopathological changes in the brain regions and the other organs after 28 days treatment (Fig. S22, ESI†). Taken together with all its advantages, we demonstrate that F-SLCOOH not only significantly reduces Aβ induced cytotoxicity in neuronal cells but also exerts neuroprotection against

the ROS generation and Aβ-induced cell death. In addition, F-SLCOOH can exert highly efficient Aβ anti-fibrillation properties even at very low concentration and effectively suppress the formation of Aβ aggregates and Aβ fibrils.

3.6. F-SLCOOH treatment promotes an autophagy flux and lysosomal biogenesis in neuronal cells

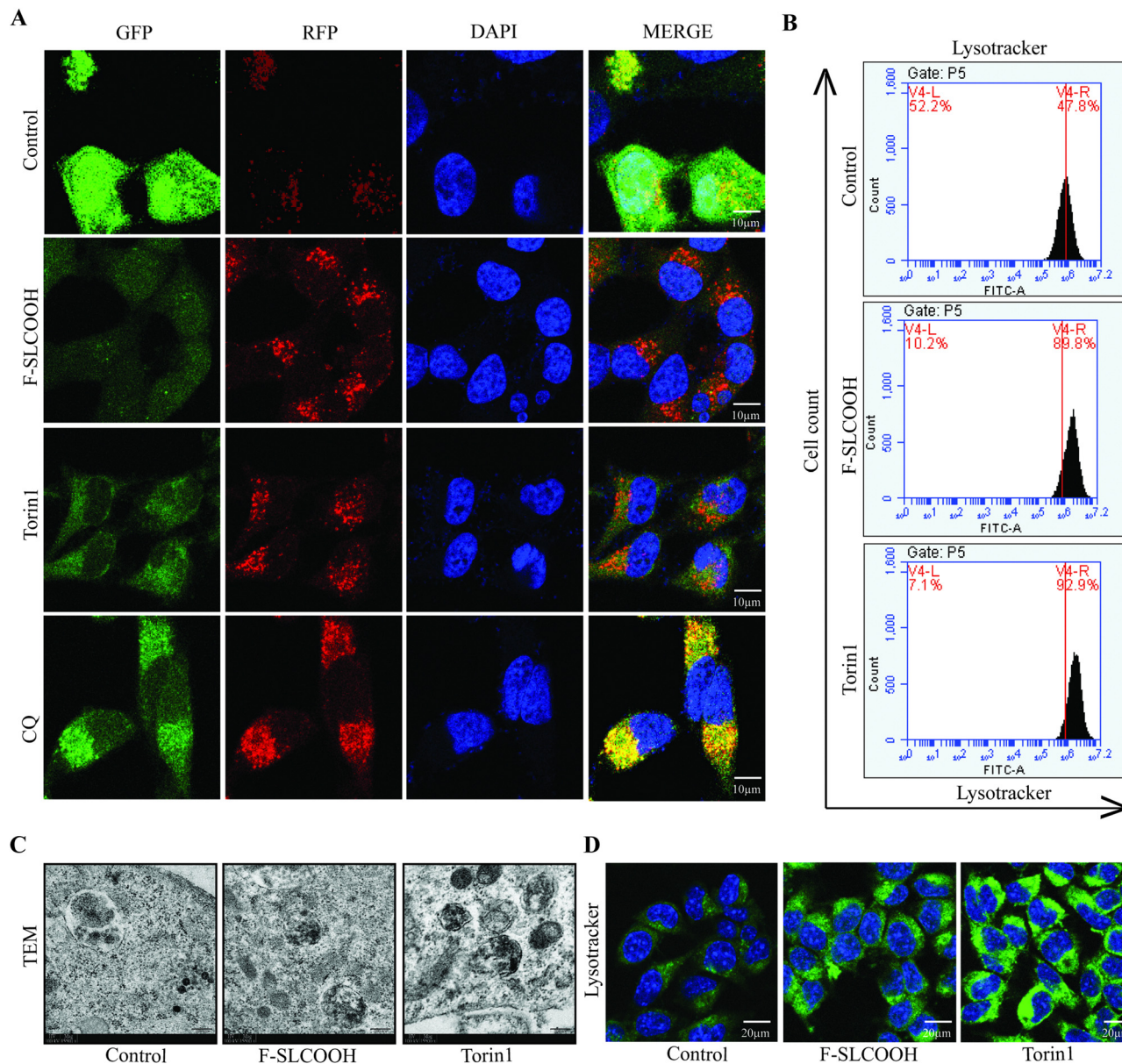In the early stages of AD, the intracellular and extracellular accumulation of toxic proteins such as Aβ aggregates and phosphorylated tau can cause disruption in the normal signalling pathways of degradation in the neuronal cells.[36–38] The canonical process of protein degradation is mainly *via* macro-autophagy, lysosomal biogenesis and lysosome or cargo transport in the neurons of the brain.[39,40] When this autophagic lysosomal pathway is highly disturbed in the early stages of the AD progression, the aggregated proteins tend to accumulate and disrupt the cell-to-cell connection causing neuronal death.[41,42] Therefore, to evaluate the efficacy of F-SLCOOH whether it can promote the lysosomal biogenesis and autophagy flux, we performed certain *in vitro* experiments in the cell models. As the first step to detecting the autophagy flux, we treated F-SLCOOH (20 μM) in HeLa cells stably over-expressing tandem fluorescent mRFP-GFP-LC3 (tfLC3), and Torin1 (250 nM) and CQ (50–100 μM), which were used as positive controls for autophagy activation and inhibition, respectively. As expected, F-SLCOOH exhibited (Fig. 6A) a good increase in autophagy flux as compared to Torin1 positive control demonstrating more RFP generation in the cells contributing to the fusion of generated autophagosomes and lysosomes for the formation of autolysosomes. We also found that F-SLCOOH treatment in the N2a neuronal cells could increase the lysosome number in the lysotracker experiment detected by using flow cytometry (Fig. 6B) as compared to that of the control, elucidating lysosomal biogenesis. These results were further confirmed by the lysotracker staining experiment, using immunocytochemistry (Fig. 6D) consistently implicating lysosomal biogenesis. Furthermore, transmission electron microscopy (TEM) images have captured and detected the autolysosomes formation in the neuronal cells. As anticipated, F-SLCOOH treatment in the N2a neuronal cells significantly increased the autolysosomes formation when compared with that of the controls and the increase of autolysosomes was comparable to that of the positive control Torin1. Collectively, the results from these experiments indicate that F-SLCOOH treatment promotes autophagy flux and lysosomal biogenesis in neuronal cells signifying that F-SLCOOH can potentially be used as a theranostic agent for neurodegenerative diseases.

4. Discussion

Fluoro-substituted cyanine has been shown to have desirable multifunctional properties for the detection, diagnosis, and therapeutics of AD,[11,32,33] especially, BBB permeability and specific Aβ targeting. These probes can be used for the early-stage detection and diagnostics of AD by specifically targeting

7552 | *J. Mater. Chem. B*, 2024, **12**, 7543–7556

This journal is © The Royal Society of Chemistry 2024

Fig. 6 F-SLCOOH treatment promotes lysosomal biogenesis in neuronal cells. (A) F-SLCOOH (20 μM) treatment in HeLa cells stably over-expressing tandem fluorescent mRFP-GFP-LC3 (tf-LC3), and Torin1 (250 nM) and CQ (50–100 μM), were used as positive controls for autophagy activation and inhibition, respectively revealing autophagy flux. (B) F-SLCOOH (20 μM) and Torin1 (250 nM) treatment increased lysotracker positive N2A cells as determined by flow cytometry compared to the control elucidating lysosomal biogenesis. (C) F-SLCOOH (20 μM) and Torin1 (250 nM) treatment increased autolysosome numbers compared to the control group in N2A cells as depicted by transmission electron microscopy. (D) F-SLCOOH (20 μM) and Torin1 (250 nM) treatment significantly increased lysotracker staining in N2A cells compared to the control elucidating lysosomal biogenesis as depicted by confocal imaging. Each data point is a representation of the mean ± SEM from 3 independent replicates.

the extracellular accumulation of Aβ in the form of Aβ plaques and Aβ oligomers.[11,20,21] Here we illustrate our newly synthesised theranostic molecule F-SLCOOH, which can bind and detect $Aβ_{1-42}$, Iowa mutation Aβ, and Dutch mutation Aβ fibrils and oligomers exhibiting enhanced emission with high affinity. Importantly, F-SLCOOH can readily cross the blood–brain barrier and show highly selective binding toward the extracellular Aβ aggregates in real-time in live animal imaging and diagnosis of a preclinical Alzheimer's disease 5XFAD mouse model (Fig. 1–4 and Fig. S17, ESI†). The molecular docking

studies have provided an insight into the unique and specific binding of F-SLCOOH with various Aβ species.

On the other hand, many studies have reported probes targeting Aβ fibrils and oligomers with good binding affinity, but none of the studies have illustrated whether they could be used in the *in vivo* animal models for further validation and whether those probes could cross blood–brain barrier is unknown.[43–45] Our study has shown that F-SLCOOH can readily pass through the blood–brain barrier in mice models and can bind to Aβ fibrils and oligomers. In addition, high

This journal is © The Royal Society of Chemistry 2024

J. Mater. Chem. B, 2024, **12**, 7543–7556 | **7553**

concentrations of F-SLCOOH in both brain and plasma of wildtype mice after intraperitoneal administration were found (Fig. S18 and S19, ESI†). The F-SLCOOH concentration was higher at 60 than 30 minutes illustrating that F-SLCOOH is highly bioavailable in the brain for its theranostic functions. The *ex vivo* confocal imaging of hippocampal brain slices indicated excellent colocalization of F-SLCOOH with Aβ positive NU1, 4G8, 6E10 A11 antibodies and THS staining dye, affirming its excellent Aβ plaque specificity and targetability (Fig. 3).

In addition, various research studies have illustrated molecular probes for Aβ specificity and binding affinity, but none of these compounds have shown therapeutic effects or theranostic properties for treatment of AD both *in vitro* and *in vivo*.[20,27,46–48] Here, we have demonstrated that F-SLCOOH exhibits desirable theranostic functions including exerting a highly efficient Aβ anti-fibrillation property even at very low concentration and effectively suppressing the formation of neurotoxic Aβ aggregates, Aβ fibrils of Iowa mutation Aβ and Dutch mutation Aβ (Fig. 5). F-SLCOOH treatment also promotes autophagy flux and lysosomal biogenesis in neuronal cells signifying its potential for use as an effective theranostic agent for neurodegenerative diseases (Fig. 6). Furthermore, F-SLCOOH not only significantly reduces Aβ induced cytotoxicity in neuronal cells but also affords neuroprotection against ROS generation and Aβ-induced cell death (Fig. S16, ESI†).

In summary, we have designed and synthesized a novel theranostic cyanine molecule, namely F-SLCOOH, which is shown to exhibit highly favourable multi-functions for the detection, diagnosis and treatment of AD. Even though we have illustrated various functions of this molecular probe, an evaluation of the chronic toxicity of F-SLCOOH in different animal models and the in-depth analysis of molecular targets in relation to the therapeutic efficacy of AD and other related diseases are still be needed for further characterization and development. To realize therapeutic applications, studies of pharmacodynamics and signalling pathway for the treatment of AD are also indispensable.

5. Conclusion

In conclusion, we have developed and demonstrated a novel theranostic agent namely, F-SLCOOH, which can be used for the applications of selective Aβ binding studies toward Aβ fibrils and Aβ oligomers with high fluorescence enhancement for diagnosis of AD. F-SLCOOH can readily cross the BBB and has high selective binding with Aβ plaques exerting bright fluorescence signals in the real time detection and diagnosis of a preclinical Alzheimer's disease mouse model. In addition, F-SLCOOH efficiently binds with Aβ plaques in the central and peripheral regions of the hippocampus in the 5XFAD brain. Meanwhile, F-SLCOOH can effectively exert Aβ anti-fibrillation properties suppressing the Aβ aggregates and Aβ fibril formation. Importantly, F-SLCOOH can not only significantly reduce Aβ induced cytotoxicity in neuronal cells but also exert neuroprotection against the ROS generation and Aβ-induced

cell death. Remarkably, F-SLCOOH treatment promotes autophagy flux and lysosomal biogenesis in neuronal cells signifying that F-SLCOOH can potentially be used as a theranostic agent for neurodegenerative diseases. In short, the current findings convincingly suggest that F-SLCOOH would be a safe theranostic small molecule for diagnosis and therapeutics of AD symptoms. For complete biological applications of this theranostic small molecule, some other pharmacokinetics and pharmacodynamics studies are still needed to be carried out to demonstrate the clinical viability of F-SLCOOH for AD therapeutics.

Author contributions

AI, XW, HZ, and KV conducted most of the assays and acquired and analyzed the data. AI, HWL, MSW, and ML conceived the project, funding, supervision and designed the study. AI, XW, HZ, KV, KL, XG, DW, SK, CS, JL, YK, RJ, ZD, HWL, MSW, and ML arranged the results and revised the manuscript. All authors have approved the final version of the manuscript.

Ethics approval

All animal experiments were approved by the Hong Kong Baptist University Committee on the Use of Human and Animal Subjects in Teaching and Research (HASC approval #HASC/ 20–21). The researchers who performed all the experiments got approval from the Department of Health for performing the animal experiments in Hong Kong under the licence (20–28) in DH/HT&A/8/2/6 Pt.1.

Data availability

All data generated or analyzed during this study are included in this published article and its ESI.†

Conflicts of interest

There are no conflicts to declare.

Acknowledgements

7554 | *J. Mater. Chem. B*, 2024, **12**, 7543–7556

This journal is © The Royal Society of Chemistry 2024

References

1 S. Norton, F. E. Matthews, D. E. Barnes, K. Yaffe and C. Brayne, Potential for primary prevention of Alzheimer's disease: an analysis of population-based data, *Lancet Neurol.*, 2014, **13**(8), 788–794.

2 A. Dhiman, M. Handa, M. Ruwali, D. P. Singh, P. Kesharwani and R. Shukla, Recent trends of natural based therapeutics for mitochondria targeting in Alzheimer's disease, *Mitochondrion*, 2022, **64**, 112–124.

3 A. Serrano-Pozo and J. H. Growdon, Is Alzheimer's Disease Risk Modifiable?, *J. Alzheimer's Dis.*, 2019, **67**(3), 795–819.

4 D. S. Knopman, D. T. Jones and M. D. Greicius, Failure to demonstrate efficacy of aducanumab: An analysis of the EMERGE and ENGAGE trials as reported by Biogen, December 2019, *Alzheimer's Dementia*, 2021, **17**(4), 696–701.

5 T. Athar, K. Al Balushi and S. A. Khan, Recent advances on drug development and emerging therapeutic agents for Alzheimer's disease, *Mol. Biol. Rep.*, 2021, **48**(7), 5629–5645.

6 Y. Zhang, Y. Li and L. Ma, Recent advances in research on Alzheimer's disease in China, *J. Clin. Neurosci.*, 2020, **81**, 43–46.

7 J. W. Lewcock, K. Schlepckow, G. Di Paolo, S. Tahirovic, K. M. Monroe and C. Haass, Emerging Microglia Biology Defines Novel Therapeutic Approaches for Alzheimer's Disease, *Neuron*, 2020, **108**(5), 801–821.

8 S. Boyko and W. K. Surewicz, Tau liquid–liquid phase separation in neurodegenerative diseases, *Trends Cell Biol.*, 2022, **32**(7), 611–623.

9 X. Wang, C. Wang, H. N. Chan, I. Ashok, S. K. Krishnamoorthi, M. Li, H. W. Li and M. S. Wong, Amyloid-beta oligomer targeted theranostic probes for in vivo NIR imaging and inhibition of self-aggregation and amyloid-beta induced ROS generation, *Talanta*, 2021, **224**, 121830.

10 X. Wang, A. Iyaswamy, D. Xu, S. Krishnamoorthi, S. G. Sreenivasmurthy, Y. Yang, Y. Li, C. Chen, M. Li, H. W. Li and M. S. Wong, Real-Time Detection and Visualization of Amyloid-beta Aggregates Induced by Hydrogen Peroxide in Cell and Mouse Models of Alzheimer's Disease, *ACS Appl. Mater. Interfaces*, 2023, **15**(1), 39–47.

11 A. Iyaswamy, X. Wang, S. Krishnamoorthi, V. Kaliamoorthy, S. G. Sreenivasmurthy, S. S. Kumar Durairajan, J. X. Song, B. C. Tong, Z. Zhu, C. F. Su, J. Liu, K. H. Cheung, J. H. Lu, J. Q. Tan, H. W. Li, M. S. Wong and M. Li, Theranostic F-SLOH mitigates Alzheimer's disease pathology involving TFEB and ameliorates cognitive functions in Alzheimer's disease models, *Redox Biol.*, 2022, **51**, 102280.

12 K. Rajasekhar, M. Chakrabarti and T. Govindaraju, Function and toxicity of amyloid beta and recent therapeutic interventions targeting amyloid beta in Alzheimer's disease, *Chem. Commun.*, 2015, **51**(70), 13434–13450.

13 M. G. Krone, A. Baumketner, S. L. Bernstein, T. Wyttenbach, N. D. Lazo, D. B. Teplow, M. T. Bowers and J. E. Shea, Effects of familial Alzheimer's disease mutations on the folding nucleation of the amyloid beta-protein, *J. Mol. Biol.*, 2008, **381**(1), 221–228.

14 A. Iyaswamy, S. K. Krishnamoorthi, H. Zhang, S. G. Sreenivasmurthy, Z. Zhu, J. Liu, C. F. Su, X. J. Guan, Z. Y. Wang, K. H. Cheung, J. X. Song, S. S. K. Durairajan and M. Li, Qingyangshen mitigates amyloid-beta and Tau aggregate defects involving PPARalpha-TFEB activation in transgenic mice of Alzheimer's disease, *Phytomedicine*, 2021, **91**, 153648.

15 X. Guan, A. Iyaswamy, S. G. Sreenivasmurthy, C. Su, Z. Zhu, J. Liu, Y. Kan, K. H. Cheung, J. Lu, J. Tan and M. Li, Mechanistic Insights into Selective Autophagy Subtypes in Alzheimer's Disease, *Int. J. Mol. Sci.*, 2022, **23**(7), 3609.

16 S. G. Sreenivasmurthy, A. Iyaswamy, S. Krishnamoorthi, R. N. Reddi, A. K. Kammala, K. Vasudevan, S. Senapati, Z. Zhu, C. F. Su, J. Liu, X. J. Guan, K. K. Chua, K. H. Cheung, H. Chen, H. J. Zhang, Y. Zhang, J. X. Song, S. S. Kumar Durairajan and M. Li, Bromo-protopine, a novel protopine derivative, alleviates tau pathology by activating chaperone-mediated autophagy for Alzheimer's disease therapy, *Front. Mol. Biosci.*, 2022, **9**, 1030534.

17 B. C. Tong, A. S. Huang, A. J. Wu, A. Iyaswamy, O. K. Ho, A. H. Kong, S. G. Sreenivasmurthy, Z. Zhu, C. Su, J. Liu, J. Song, M. Li and K. H. Cheung, Tetrandrine ameliorates cognitive deficits and mitigates tau aggregation in cell and animal models of tauopathies, *J. Biomed. Sci.*, 2022, **29**(1), 85.

18 C. Z. Cai, X. X. Zhuang, Q. Zhu, M. Y. Wu, H. Su, X. J. Wang, A. Iyaswamy, Z. Yue, Q. Wang, B. Zhang, Y. Xue, J. Tan, M. Li, H. He and J. H. Lu, Enhancing autophagy maturation with CCZ1-MON1A complex alleviates neuropathology and memory defects in Alzheimer disease models, *Theranostics*, 2022, **12**(4), 1738–1755.

19 C. Chen, X. Wang, D. Xu, H. Zhang, H. N. Chan, Z. Zhan, S. Jia, Q. Song, G. Song, H. W. Li and M. S. Wong, Multi-functional theranostic carbazole-based cyanine for real-time imaging of amyloid-beta and therapeutic treatment of multiple pathologies in Alzheimer's disease, *J. Mater. Chem. B*, 2023, **11**(22), 4865–4873.

20 C. L. Teoh, D. Su, S. Sahu, S. W. Yun, E. Drummond, F. Prelli, S. Lim, S. Cho, S. Ham, T. Wisniewski and Y. T. Chang, Chemical Fluorescent Probe for Detection of Abeta Oligomers, *J. Am. Chem. Soc.*, 2015, **137**(42), 13503–13509.

21 Y. Zhang, C. Ding, C. Li and X. Wang, Advances in fluorescent probes for detection and imaging of amyloid-beta peptides in Alzheimer's disease, *Adv. Clin. Chem.*, 2021, **103**, 135–190.

22 A. Aliyan, N. P. Cook and A. A. Marti, Interrogating Amyloid Aggregates using Fluorescent Probes, *Chem. Rev.*, 2019, **119**(23), 11819–11856.

23 J. Zhou, P. Jangili, S. Son, M. S. Ji, M. Won and J. S. Kim, Fluorescent Diagnostic Probes in Neurodegenerative Diseases, *Adv. Mater.*, 2020, **32**(51), e2001945.

24 K. Rajasekhar, N. Narayanaswamy, N. A. Murugan, G. Kuang, H. Agren and T. Govindaraju, A High Affinity Red Fluorescence and Colorimetric Probe for Amyloid beta Aggregates, *Sci. Rep.*, 2016, **6**, 23668.

This journal is © The Royal Society of Chemistry 2024

J. Mater. Chem. B, 2024, **12**, 7543–7556 | 7555

25 M. Ramesh and T. Govindaraju, Multipronged diagnostic and therapeutic strategies for Alzheimer's disease, *Chem. Sci.*, 2022, **13**(46), 13657–13689.

26 K. Rajasekhar, N. Narayanaswamy, N. A. Murugan, K. Viccaro, H. G. Lee, K. Shah and T. Govindaraju, Abeta plaque-selective NIR fluorescence probe to differentiate Alzheimer's disease from tauopathies, *Biosens. Bioelectron.*, 2017, **98**, 54–61.

27 N. Yue, H. Fu, Y. Chen, X. Gao, J. Dai and M. Cui, Rational design of molecular rotor-based fluorescent probes with bi-aromatic rings for efficient in vivo detection of amyloid-beta plaques in Alzheimer's disease, *Eur. J. Med. Chem.*, 2022, **243**, 114715.

28 M. Zhang, H. Fu, W. Hu, J. Leng and Y. Zhang, Versatile Dicyanomethylene-Based Fluorescent Probes for the Detection of beta-Amyloid in Alzheimer's Disease: A Theoretical Perspective, *Int. J. Mol. Sci.*, 2022, **23**(15), 8619.

29 S. Pratihar, K. K. Bhagavath and T. Govindaraju, Small molecules and conjugates as theranostic agents, *RSC Chem. Biol.*, 2023, **4**(11), 826–849.

30 F. Gao, J. Chen, Y. Zhou, L. Cheng, M. Hu and X. Wang, Recent progress of small-molecule-based theranostic agents in Alzheimer's disease, *RSC Med. Chem.*, 2023, **14**(11), 2231–2245.

31 Y. Li, D. Xu, S. L. Ho, H. W. Li, R. Yang and M. S. Wong, A theranostic agent for in vivo near-infrared imaging of beta-amyloid species and inhibition of beta-amyloid aggregation, *Biomaterials*, 2016, **94**, 84–92.

32 Y. Li, D. Xu, A. Sun, S. L. Ho, C. Y. Poon, H. N. Chan, O. T. W. Ng, K. K. L. Yung, H. Yan, H. W. Li and M. S. Wong, Fluoro-substituted cyanine for reliable in vivo labelling of amyloid-beta oligomers and neuroprotection against amyloid-beta induced toxicity, *Chem. Sci.*, 2017, **8**(12), 8279–8284.

33 X. Wang, H. N. Chan, N. Desbois, C. P. Gros, F. Bolze, Y. Li, H. W. Li and M. S. Wong, Multimodal Theranostic Cyanine-Conjugated Gadolinium(III) Complex for In Vivo Imaging of Amyloid-beta in an Alzheimer's Disease Mouse Model, *ACS Appl. Mater. Interfaces*, 2021, **13**(16), 18525–18532.

34 C. Peng, X. Wang, Y. Li, H. W. Li and M. S. Wong, Versatile fluorescent probes for near-infrared imaging of amyloid-beta species in Alzheimer's disease mouse model, *J. Mater. Chem. B*, 2019, **7**(12), 1986–1995.

35 A. Iyaswamy, K. Vasudevan, S. Jayaraman, R. Jaganathan, A. Thakur, R. C. Chang and C. Yang, Editorial: Advances in Alzheimer's disease diagnostics, brain delivery systems, and therapeutics, *Front. Mol. Biosci.*, 2023, **10**, 1162879.

36 K. Selvarasu, A. K. Singh, A. Dakshinamoorthy, S. G. Sreenivasmurthy, A. Iyaswamy, M. Radhakrishnan, S. Patnaik, J. D. Huang, L. L. Williams, S. Senapati and S. S. K. Durairajan, Interaction of Tau with Kinesin-1: Effect of Kinesin-1 Heavy Chain Elimination on Autophagy-Mediated Mutant Tau Degradation, *Biomedicines*, 2023, **12**(1), 5.

37 A. Iyaswamy, K. Lu, X. J. Guan, Y. Kan, C. Su, J. Liu, R. Jaganathan, K. Vasudevan, J. Paul, A. Thakur and M. Li, Impact and Advances in the Role of Bacterial Extracellular Vesicles in Neurodegenerative Disease and Its Therapeutics, *Biomedicines*, 2023, **11**(7), 2056.

38 S. Krishnamoorthi, A. Iyaswamy, S. G. Sreenivasmurthy, A. Thakur, K. Vasudevan, G. Kumar, X. J. Guan, K. Lu, I. Gaurav, C. F. Su, Z. Zhu, J. Liu, Y. Kan, S. Jayaraman, Z. Deng, K. K. Chua, K. H. Cheung, Z. Yang, J. X. Song and M. Li, PPARa Ligand Caudatin Improves Cognitive Functions and Mitigates Alzheimer's Disease Defects By Inducing Autophagy in Mice Models, *J. Neuroimmune Pharmacol.*, 2023, **18**(3), 509–528.

39 A. Iyaswamy, A. Thakur, X. J. Guan, S. Krishnamoorthi, T. Y. Fung, K. Lu, I. Gaurav, Z. Yang, C. F. Su, K. F. Lau, K. Zhang, R. C. Ng, Q. Lian, K. H. Cheung, K. Ye, H. J. Chen and M. Li, Fe65-engineered neuronal exosomes encapsulating corynoxine-B ameliorate cognition and pathology of Alzheimer's disease, *Signal Transduction Targeted Ther.*, 2023, **8**(1), 404.

40 X. J. Guan, Z. Q. Deng, J. Liu, C. F. Su, B. C. Tong, Z. Zhu, S. G. Sreenivasmurthy, Y. X. Kan, K. J. Lu, C. P. Chu, R. B. Pi, K. H. Cheung, A. Iyaswamy, J. X. Song and M. Li, Corynoxine promotes TFEB/TFE3-mediated autophagy and alleviates Abeta pathology in Alzheimer's disease models, *Acta Pharmacol. Sin.*, 2024, **45**(5), 900–913.

41 A. Pandaram, J. Paul, W. Wankhar, A. Thakur, S. Verma, K. Vasudevan, D. Wankhar, A. K. Kammala, P. Sharma, R. Jaganathan, A. Iyaswamy and R. Rajan, Aspartame Causes Developmental Defects and Teratogenicity in Zebra Fish Embryo: Role of Impaired SIRT1/FOXO3a Axis in Neuron Cells, *Biomedicines*, 2024, **12**(4), 855.

42 J. Yang, W. Zhang, S. Zhang, A. Iyaswamy, J. Sun, J. Wang and C. Yang, Novel Insight into Functions of Transcription Factor EB (TFEB) in Alzheimer's Disease and Parkinson's Disease, *Aging Dis.*, 2023, **14**(3), 652–669.

43 Z. Liu, X. Li, X. Wu and C. Zhu, A dual-inhibitor system for the effective antifibrillation of Abeta40 peptides by biodegradable EGCG-Fe(iii)/PVP nanoparticles, *J. Mater. Chem. B*, 2019, **7**(8), 1292–1299.

44 G. T. Heller, F. A. Aprile, T. C. T. Michaels, R. Limbocker, M. Perni, F. S. Ruggeri, B. Mannini, T. Lohr, M. Bonomi, C. Camilloni, A. De Simone, I. C. Felli, R. Pierattelli, T. P. J. Knowles, C. M. Dobson and M. Vendruscolo, Small-molecule sequestration of amyloid-beta as a drug discovery strategy for Alzheimer's disease, *Sci. Adv.*, 2020, **6**(45), eabb5924.

45 S. S. Durairajan, Q. Yuan, L. Xie, W. S. Chan, W. F. Kum, I. Koo, C. Liu, Y. Song, J. D. Huang, W. L. Klein and M. Li, Salvianolic acid B inhibits Abeta fibril formation and disaggregates preformed fibrils and protects against Abeta-induced cytotoxicty, *Neurochem. Int.*, 2008, **52**(4–5), 741–750.

46 S. Kim, H. J. Lee, E. Nam, D. Jeong, J. Cho, M. H. Lim and Y. You, Tailoring Hydrophobic Interactions between Probes and Amyloid-beta Peptides for Fluorescent Monitoring of Amyloid-beta Aggregation, *ACS Omega*, 2018, **3**(5), 5141–5154.

47 Y. Hu, B. Su, H. Zheng and J. R. Kim, A peptide probe for detection of various beta-amyloid oligomers, *Mol. BioSyst.*, 2012, **8**(10), 2741–2752.

48 J. Yang, B. Zhu, W. Yin, Z. Han, C. Zheng, P. Wang and C. Ran, Differentiating Abeta40 and Abeta42 in amyloid plaques with a small molecule fluorescence probe, *Chem. Sci.*, 2020, **11**(20), 5238–5245.

7556 | *J. Mater. Chem. B*, 2024, **12**, 7543–7556

This journal is © The Royal Society of Chemistry 2024